



HAL
open science

Intercomparison of tropical tropospheric humidity in GCMs with AMSU-B water vapor data

Hélène Brogniez, Raymond T. Pierrehumbert

► **To cite this version:**

Hélène Brogniez, Raymond T. Pierrehumbert. Intercomparison of tropical tropospheric humidity in GCMs with AMSU-B water vapor data. *Geophysical Research Letters*, 2007, 34 (17), 10.1029/2006GL029118 . insu-02153945

HAL Id: insu-02153945

<https://insu.hal.science/insu-02153945>

Submitted on 5 Mar 2021

HAL is a multi-disciplinary open access archive for the deposit and dissemination of scientific research documents, whether they are published or not. The documents may come from teaching and research institutions in France or abroad, or from public or private research centers.

L'archive ouverte pluridisciplinaire **HAL**, est destinée au dépôt et à la diffusion de documents scientifiques de niveau recherche, publiés ou non, émanant des établissements d'enseignement et de recherche français ou étrangers, des laboratoires publics ou privés.



Intercomparison of tropical tropospheric humidity in GCMs with AMSU-B water vapor data

Hélène Brogniez^{1,2} and Raymond T. Pierrehumbert¹

Received 18 December 2006; revised 11 June 2007; accepted 6 August 2007; published 12 September 2007.

[1] We make use of microwave measurements of the tropical free tropospheric relative humidity (FTH) to evaluate the extent to which the water vapor distribution in four general circulation models is faithful to reality. The comparison is performed in the tropics by sorting the FTH in dynamical regimes defined upon the 500 hPa vertical velocity. Because microwave radiation penetrates non-rainy and warm clouds, we are able to estimate the FTH over most of the dynamical regimes that characterize the tropics. The comparisons reveal that two models simulate a free troposphere drier than observed (<10%), while the others agree with the observations. Despite some differences, the level of agreement is good enough to lend confidence in the representation of atmospheric moistening processes. A climate change scenario, tested on two models, shows a tendency to maintain the FTH to an almost fixed value be it an ascending or a subsiding regime. **Citation:** Brogniez, H., and R. T. Pierrehumbert (2007), Intercomparison of tropical tropospheric humidity in GCMs with AMSU-B water vapor data, *Geophys. Res. Lett.*, *34*, L17812, doi:10.1029/2006GL029118.

1. Introduction

[2] The generally accepted view of climate sensitivity states that the warming of the troposphere induced by an increase of the greenhouse effect should yield an increase of the water vapor concentration. While in the boundary layer such increase is directly related to the increase of surface temperature (via Clausius-Clapeyron), this link is less straightforward in the free troposphere [Minschwaner and Dessler, 2004]. The sensitivity of the outgoing longwave radiation to water vapor perturbations has led to a focus on the free tropospheric water vapor (roughly 100–700 hPa), water vapor in the boundary-layer having a less significant effect on the global feedback [Spencer and Braswell, 1997; Held and Soden, 2000]. We focus here on the tropical atmosphere using observations and simulations of the free tropospheric relative humidity (FTH) realized at microwave frequencies. Since microwave radiation penetrates most of the clouds, except cold and/or rainy clouds such as cumulus found in monsoonal regions, the comparisons can be performed over most of the tropics, the use of infrared data limiting such retrievals to cloud free regions [Brogniez et al., 2005].

[3] The distribution of FTH in the tropical belt is controlled by the Hadley-Walker circulation and by lateral mixing [Sherwood, 1996; Pierrehumbert, 1998], the main supply of moisture in the tropical atmosphere being the convection of the Inter-Tropical Convergence Zone. Faithful simulation of water vapor involves the simulation of large-scale dynamical features [Emanuel and Pierrehumbert, 1996], as well as convection [Frierson, 2007] and microphysical processes in clouds [Emanuel and Živković-Rothman, 1999]. Uncertainties in the latter processes make it particularly important to evaluate the behavior of models in cloudy convective regions.

[4] With the availability of more than 20 years of satellite observations of FTH, there has been an increased effort to assess its representation in climate models up to decadal time scales. Hence, while a large majority of climate models tend to simulate correctly the main features of the tropical distribution of water vapor, with a fairly good representation of the phase and amplitude of the seasonal cycle of cloud free areas [Brogniez et al., 2005; Gettelman et al., 2006], substantial biases have been highlighted at the interannual and mean seasonal scales [Allan et al., 2003]. Among the major suggested problems are the strength of the overturning tropical circulation (e.g., too vigorous in the HadAM3 model [Allan et al., 2003]), large-scale mechanisms related to moisture export from convective areas, and the representation of convection.

[5] The use of microwave data to diagnose the FTH in cloudy regions should help to improve the representation of the microphysical processes that yield the distribution and variability of the tropospheric water vapor.

[6] Despite the aforementioned biases and differences in the schemes used to parameterize sub-grid processes, there is general agreement amongst models that the water vapor feedback should amplify by about a factor of two the sensitivity of climate to an increase of the greenhouse gases concentration [e.g., Cess et al., 1990; Held and Soden, 2000]. Trend studies show little variations (a few percents) of the free tropospheric relative humidity on interannual to decadal timescales [Soden et al., 2005]. In fact, recent analyses based on climate models suggest that under a warming climate, the water vapor feedback is characterized by an approximately fixed atmospheric relative humidity [Larson and Hartmann, 2003; Bony et al., 2006; Soden and Held, 2006].

[7] The central goal of this study is the comparison of the simulated present tropical climate with observations, extending previous studies on the matter to most of the cloudy regions. Section 2 describes the compositing approach used to sort the tropical atmosphere into dynamical regimes. The results of this method applied to four coupled GCMs are then discussed in section 3 with a first analysis of

¹Department of Geophysical Sciences, University of Chicago, Chicago, Illinois, USA.

²Now at Centre d'Etude des Environnements Terrestres et Planétaires, CNRS, IPSL, Velizy, France.

a climate change projection. Section 4 summarizes the main findings of the study.

2. Data and Methods

[8] This study is based on the decomposition of the large-scale tropical circulation into dynamical regimes proposed by *Bony et al.* [2004]. This method uses the mid-tropospheric vertical velocity ω_{500} as a proxy for the vertical motions of the tropical atmosphere. It has the advantages of focusing on the evolution of a particular regime (ascending, subsiding), in terms of its frequency of occurrence, and on the associated atmospheric variable. Therefore biases in the simulation of the dynamical patterns do not affect the model-data comparison. Here this framework allows the study of perturbations induced by a climate change on the FTH distribution in a given dynamical situation. The tropical atmosphere is discretized into finite ω_{500} regimes (intervals of 10 hPa/day) such as the probability distribution function P_ω of ω_{500} over the entire range is normalized to unity. Thanks to this discretization of the troposphere, the mean perturbation $\overline{\delta FTH}$, averaged over the domain (30°N–30°S) can be computed in the form

$$\overline{\delta FTH} = \int_{-\infty}^{+\infty} FTH_\omega \delta P_\omega d\omega + \int_{-\infty}^{+\infty} P_\omega \delta FTH_\omega d\omega + \int_{-\infty}^{+\infty} \delta FTH_\omega \delta P_\omega d\omega$$

Following *Bony et al.* [2004] these terms are referred to as the dynamic component ($FTH\delta P$), which describes the perturbation on FTH due to circulation changes only, the thermodynamic component ($P\delta FTH$), which describes the part of $\overline{\delta FTH}$ that does not result directly from circulation changes (e.g. temperature lapse rate variations), and a co-variation component ($\delta FTH\delta P$).

[9] The same statistical technique is applied to the observations and to models simulations. We use two independent sets of meteorological reanalysis to build the observed monthly mean ω_{500} : the NCEP/DOE AMIP-II (NCEP2) reanalysis produced at NOAA (2.5°) [*Kanamitsu et al.*, 2002] and the ERA-40 reanalysis from the ECMWF (1.125°) [*Uppala et al.*, 2005]. The reference ω_{500} is then collocated with the observed FTH derived from the observations in the 183.31 ± 1 GHz water vapor channel of the Advanced Microwave Sounding Unit-B (AMSU-B), onboard the NOAA satellites. This channel provides measurements of the water vapor of the free troposphere, roughly between 700 and 200 hPa, the actual width of the layer depending upon the humidity content and, to a lesser extent, the temperature profile. While non-rainy and warm clouds do not affect the measured radiation, a mask was applied to remove the precipitating [*Greenwald and Christopher*, 2002] and deep convective [*Hong et al.*, 2005] clouds using the complimentary measurements of the other AMSU-B channels [see also *Brogniez and Pierrehumbert*, 2006]. Hence, all known cloud bias is removed in the observational dataset. The data are then interpreted in terms of FTH using the log-linear relationship $\ln RH = a \cdot BT + b$, for limb-corrected observations [*Soden and Bretherton*, 1993]. In this equation \overline{RH} is the layer-mean relative humidity weighted by the relative humidity jacobian, i.e. the FTH,

BT is the 183.31 ± 1 GHz brightness temperature (in Kelvins), and a and b (resp. -0.0887 K^{-1} and 25.43) are fitting coefficients obtained from a training dataset representative of the observed tropical atmosphere [*Brogniez et al.*, 2005]. The observed FTH is retrieved for November and December 2001 (NOAA-16 platform), regrided from the 16 km footprint at nadir to a regular 0.5° grid, and averaged over time to perform the comparison with ω_{500} at the monthly time scale.

[10] Beside the FOAM (The FOAM GCM is a portable, Beowulf-oriented re-implementation of the NCAR Community Climate Model-3. It has the atmospheric physic of CCM3. See <http://www-unix.mcs.anl.gov/foam/index.html> for further details.) model developed at the University of Chicago, and the Coupled Model version 4 developed at the Institut Pierre Simon Laplace (IPSL-CM4), the two other models were chosen based on completeness of data availability (3-D fields of daily temperature and specific humidity and of monthly vertical velocity) at the Program for Climate Model Diagnosis and Intercomparison archive. Those two models are: the Max Planck Institute for Meteorology 5th-generation atmospheric general circulation model (ECHAM5); the Model for Interdisciplinary Research on Climate, version 3.2 high resolution, from the Center for Climate System Research, University of Tokyo (MIROC3.2).

[11] The models have different spatial resolutions and different physical parametrization schemes: FOAM was run at the $4.5^\circ \times 7.5^\circ$ resolution, is coupled to a slab ocean, uses a relative humidity-based cloud scheme and the deep convection follows a plume ensemble concept [*Zhang and McFarlane*, 1995]; ECHAM5 is on a 1.865° grid, is coupled to a slab ocean, uses a prognostic cloud scheme and the deep convection is parameterized using the mass-flux scheme of *Tiedtke* [1989] with adjustment-type closure; MIROC3.2 has a 1.125° grid, is also coupled to a slab ocean, uses also a prognostic cloud scheme and the deep convection is according to the cumulus scheme from *Arakawa and Schubert* [1974] together with a threshold on the ambient relative humidity; finally IPSL-CM4 has a $3.5^\circ \times 2.5^\circ$ resolution, is the only model of the set coupled to a fully resolved ocean, uses a statistical cloud scheme and the moist convection is treated according to *Emanuel* [1991]. The advection of passive tracers (such as vapor, liquid and solid water) is modeled by a finite volume scheme in the IPSL-CM4 model and by semi-lagrangian schemes in FOAM, ECHAM5 and MIROC3.2. One needs to note here that outputs from ECHAM5 and MIROC3.2 are provided on 9 pressure levels (ranging from 1000 to 200 hPa; IPCC output convention), whereas outputs from FOAM and IPSL-CM4 are provided on 19 sigma-pressure levels (ranging from 1000 to 10 hPa). Such difference in the vertical resolution can lead up to a 1.2 K difference on the BT, computed for a standard tropical atmosphere, which translates into a relative dry bias $\Delta FTH/FTH \simeq -10\%$ ($FTH_{19 \text{ lev}} < FTH_{9 \text{ lev}}$), that could explain only a relatively small part of the observed biases (see section 3). For each GCM, the control experiment is based on the actual atmospheric CO_2 concentration (370 ppm in 2001), except for IPSL-CM4 that uses pre-industrial CO_2 concentration (280 ppm in 1860). The climate change experiments for

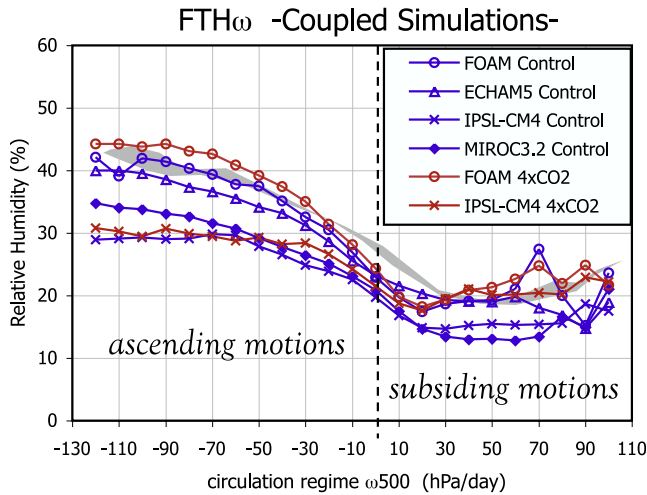


Figure 1. Composite FTH_{ω} of FTH in the different circulation regimes ω_{500} . The shaded area represents the observed FTH (AMSU-B) and its standard deviation, defined from the differences in ω_{500} between the two re-analysis datasets (NCEP/NCAR and ERA40). The blue lines represent the control experiments and the red lines represent the climate change experiments.

FOAM and IPSL-CM4 discussed in section 4 are based on 4 times the control CO_2 concentrations.

[12] The evaluations are based on the “model-to-satellite” approach. Here we use the RTTOV-8 radiative code to compute the 183.31 ± 1 GHz BT from the outputs (temperature and specific humidity) [Matricardi *et al.*, 2004]. Thus, if an uncertainty can be reasonably expected from the radiative transfer simulation (due to the representation of microphysics and scattering for instance), this uncertainty is propagated among the whole set of models. However, because no cloud profile information (cloud liquid and ice water paths, cloud fraction) was available at the required daily frequency, the possible effects of scattering by deep convective clouds on the microwave BT were not included. Since such clouds are associated to the strongest ascending regimes ($\omega_{500} < -50$ hPa/day, [Bony *et al.*, 2004]), the comparisons between models and data, discussed in the following, are done only for those regimes for which the BT is not affected by convective clouds ($\omega_{500} > -50$ hPa/day). This permits a consistent inter-model comparison, though the possibility remains that comparisons with AMSU-B data may be compromised by biases caused by remaining scattering effects in the cloudy regions (Figure 1). Finally, the FTH is retrieved from the simulated BT using the same coefficients as in the observations thus minimizing the bias due to the retrieval algorithm. To be consistent with the available observation dataset, we considered only two months from one year (November and December) from each model. The results presented below were checked against an additional year of data, to verify that the chosen period was not anomalous.

3. Results and Discussion

[13] We first consider the vertical velocity fields used to decompose the atmospheric circulation. As expected from

previous work [Bony *et al.*, 2004], the probability distribution functions P_{ω} of ω_{500} (not shown, see Bony *et al.* [2004, Figure 5]) have a maximum around 15–20 hPa/day that is consistent among the GCMs and with the observed P_{ω} and that represents the large area of the Tropics dominated by moderate subsidence.

[14] The water vapor fields are evaluated by comparing the satellite-derived FTH and the modeled FTH. The FTH is used to evaluate the simulated water vapor because it provides a convenient vertical average diagnostic of the radiatively important part of the water vapor field. Moreover, in the framework of climate change analyses, such a diagnostic can be used to relate the discussion to previous discussions on the question and to predict what should be observed by the satellites in the coming decades. The link between the FTH and the large-scale vertical velocity is explicitly described in Figure 1. Thanks to the use of microwave data, the comparisons are performed over most of the dynamical regimes of the Tropics, including the ones associated with cloudiness. The models’ FTH distribution shows some differences with respect to the observed one. Hence, FOAM produces a control run similar to the observations, while ECHAM5 shows a slight dry bias of 2–3% within the ascending regions. IPSL-CM4 and MIROC3.2 reveal a more important underestimation that reaches 5% in the clear sky subsiding areas and up to 10% in the ascent regimes. The pronounced gradient that separates the strongly ascending motions from the strongly subsiding motions in the observations seems to be correctly reproduced by the four models, albeit slightly steeper in FOAM.

[15] Microphysics and the large-scale circulation are both potentially involved in the biases found here. On the one hand, since the circulation of the atmosphere exerts a strong influence on the distribution of water vapor, the biases highlighted in the cloud-free subsiding areas, suggest problems in the horizontal mixing that links subtropical areas to convective regions [Pierrehumbert, 1998], and in the outflows from clouds. It is also possible that biases regarding shallow convection are playing a role. On the other hand, the biases highlighted in the ascent regimes and part of the bias of the subsiding regimes presumably reflect problems with the representation of the moistening of the atmosphere by convective systems. Thus the overall dry bias of the IPSL-CM4 and MIROC3.2 control simulations suggests that their convection schemes might have a higher precipitation efficiency than that of FOAM and ECHAM5 (for the ascending areas), leaving too little condensate to moisten the atmosphere, and that their large-scale transport might be too strong (for the subsiding areas). Using a single-column model, Emanuel and Živković-Rothman [1999] suggested that low sensitivity to microphysics was an artifact of low vertical resolution, while Ingram [2002] revealed that the water vapor feedback in a full GCM remains insensitive to microphysics even at high vertical resolution (see Sherwood and Meyer [2006] for related results in an idealized model) which tend to be supported by our results.

[16] This framework is then used to provide insight onto the representation of the water vapor feedback. We use quadrupled CO_2 concentration scenarios produced by FOAM and IPSL-CM4. As seen in Figure 1, the two models reveal a similar behavior under a warming situation with the

Table 1. Equilibrium Sensitivities of Global Mean Surface Temperature and Decomposition into Dynamic, Thermodynamic, and Co-Variation Components, of the Tropically Average Change in FTH ($\overline{\delta FTH}$) for the FOAM and IPSL-CM4 Models

	ΔT , K	$\overline{\delta FTH}$			
		Total, %	Dynamic, %	Thermodynamic, %	Co-Variation, %
FOAM	2.75	1.5	0.27	1.24	-0.01
IPSL-CM4	2.89	2.3	0.0	2.44	-0.14

prediction that the FTH distribution should remain almost constant between the climate change scenario and the control one. Slight differences can be noticed: FOAM simulates a small increase in the relative humidity, suggesting a stronger water vapor feedback than would be yielded by fixed FTH, lying between 3% (ascent) and 1% (descent) while IPSL-CM4 proposes a more contrasted response, with an almost null difference in the ascending regimes and a increase of FTH reaching about 5% in the subsiding regions. Thus, even though the previous analysis reveals some major differences in the representation of the base-state humidity of the cloudy atmosphere by these two models, this does not imply corresponding differences in the simulation of the FTH response to climate change. Indeed, a model that keeps FTH fixed in the course of warming will give approximately the same water vapor feedback whether the fixed FTH is 10% or 20%. This is so because the radiative effect of water vapor is roughly logarithmic in the absolute humidity [Held and Soden, 2000; Pierrehumbert *et al.*, 2007].

[17] The differences in P_ω (not shown) are consistent with the findings of Wyant *et al.* [2006] and Bony *et al.* [2004]: the forcing results in an overall slight weakening of the large-scale overturning circulation with an increase of the frequency of the moderate regimes ($-30 \leq \omega_{500} \leq$

20 hPa/day) while the frequencies of strong convective and strong subsiding situations slightly decrease. Such result appears to be a robust consequence of energetic constraints on the hydrological cycle in global warming simulations. The dynamic and thermodynamic contributions to the mean change in tropical FTH (Table 1) reveal that the slowdown of the tropical circulation has a negligible effect on the free tropospheric relative humidity, which differs from the moistening expected from such modification of the circulation.

[18] The impact of such FTH changes on the outgoing longwave radiation (OLR) is presented in Figure 2. The moistening patterns that show up for the two models are associated with a reduction of the OLR, while an increase of the OLR is generally associated with drier areas. The offset between those regions of enhanced or reduced water vapor feedback seems more pronounced for IPSL-CM4, while its climate sensitivity is roughly similar to FOAM's (Table 1). Finally the decomposition into dynamic and thermodynamic contributions (Table 1) suggests that for both models the changes of the tropical FTH ($\overline{\delta FTH}$) are dominated by thermodynamic changes, dynamic changes accounting for small contributions.

4. Summary

[19] Understanding, quantifying, and representing an accurate water vapor feedback are central to any model prediction of climate change. GCMs are essentially all in agreement with respect to the strength of the water vapor feedback [Soden and Held, 2006]. As our results show, however, this does not mean that all GCMs accomplish the feedback in the same way. Models vary with regard to their biases vis a vis observations, but the approximately logarithmic dependence of radiation on water vapor limits the impact of the biases. While there are noticeable differences in the schemes used in the present GCMs (convection schemes, treatment of cloud microphysics), the comparison

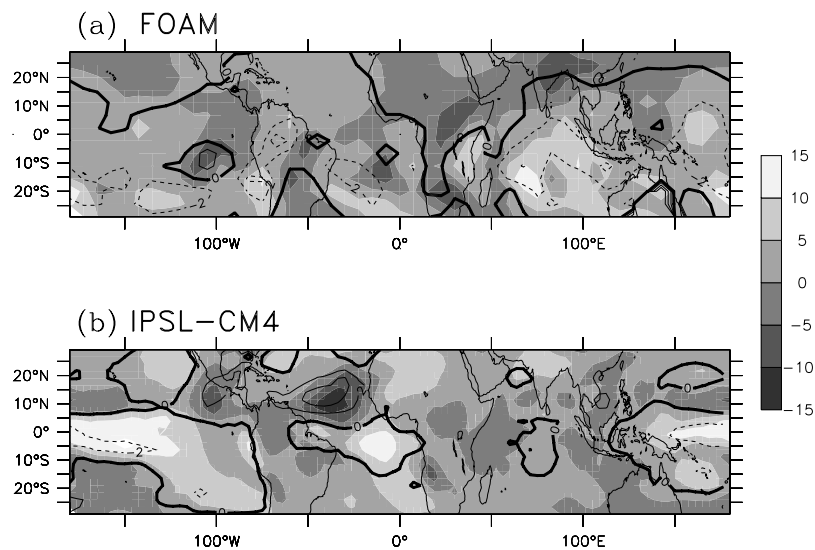


Figure 2. Maps of the differences of FTH (in %) between the climate change and the control experiments for (a) the FOAM model and (b) the IPSL-CM4 model. The overlaying contours represent the sensitivity of the clear-sky outgoing longwave radiation to a change in the surface temperature ($dOLR/dT$, in $W/m^2/K$). The dashed contours represent negative values and the interval between contours is $2 W/m^2/K$.

shows that they capture the water vapor distribution even in the convective regions where simulation of water vapor is most problematic. Thanks to microwave data, this study extends the analyses made in the mid-latitudes [Brogniez and Pierrehumbert, 2006] and in the tropical clear sky zones [Pierrehumbert, 1998; Soden et al., 2005] to the cloudy regions. Questions still remain about the sensitivity of the water vapor field to climate forcing and the effect of the changes of the water vapor field on the climate sensitivity. The additional insight provided on the behavior of a subset of GCMs under warming, maintaining the free tropospheric humidity to an almost fixed value, seems to agree with the findings of Sherwood and Meyer [2006]: the sensitivity of the water vapor feedback, as currently described, to the representation of cloud microphysics does not seem to exceed a few percents. However, despite the generally good agreement in convective regions, one cannot strictly rule out the possibility that microphysics as currently implemented responds incorrectly to a warming climate. This is especially the case given that the microphysical parameterizations were formulated before the availability of microwave FTH retrievals, and therefore could not have been tuned to such data. To be confirmed, such analysis needs to be extended to a larger set of models and this will be the object of future studies.

[20] **Acknowledgments.** We first acknowledge the two anonymous reviewers for their constructive and valuable comments which led to an improved version of the manuscript. We also acknowledge the international modeling groups for providing their data for analysis, the Program for Climate Model Diagnosis and Intercomparison (PCMDI) for collecting and archiving the model data, the Climate Variability Predictability Project Joint Scientific Committee (JSC/CLIVAR) Working Group on Coupled Modeling (WGCM) for organizing the model analysis activity. The Intergovernmental Panel on Climate Change (IPCC) Working Group 1 Technical Support Unit for technical support. The IPCC Data Archive at Lawrence Livermore National Laboratory is supported by the Office of Science, U.S. Department of Energy. We finally thank the Institut Pierre Simon Laplace and S. Denvil in particular for his help on the IPSL-CM4 outputs. The AMSU-B data comes from the Comprehensive Large Array-data Stewardship System (CLASS) of the NOAA-NESDIS and was processed using the AAPP software distributed by the Numerical Weather Prediction-Service Application Facilities (MetOffice, Eumetsat, KNMI, MétéoFrance). This work was funded by the National Science Foundation under grants ATM-0123999 and ATM-0121028.

References

Allan, R. P., M. A. Ringer, and A. Slingo (2003), Evaluation of moisture in the Hadley Center climate model using simulations of HIRS water-vapor channel radiances, *Q. J. R. Meteorol. Soc.*, **129**, 3371–3389.

Arakawa, A., and W. H. Schubert (1974), Interaction of a cumulus cloud ensemble with the large-scale environment, *J. Atmos. Sci.*, **31**, 674–701.

Bony, S., J.-L. Dufresne, H. LeTreut, J.-J. Morcrette, and C. Senior (2004), On dynamic and thermodynamic components of cloud changes, *Clim. Dyn.*, **22**, 71–86.

Bony, S., et al. (2006), How well do we understand and evaluate climate change feedback processes?, *J. Clim.*, **19**, 3445–3482.

Brogniez, H., and R. T. Pierrehumbert (2006), Using microwave observations to assess large-scale control of free tropospheric water vapor in the mid-latitudes, *Geophys. Res. Lett.*, **33**, L14801, doi:10.1029/2006GL026240.

Brogniez, H., R. Roca, and L. Picon (2005), Evaluation of the distribution of subtropical free tropospheric humidity in AMIP-2 simulations using METEOSAT water vapor channel data, *Geophys. Res. Lett.*, **32**, L19708, doi:10.1029/2005GL024341.

Cess, R., et al. (1990), Intercomparison and interpretation of climate feedback processes in 19 atmospheric general circulation models, *J. Geophys. Res.*, **95**, 16,601–16,615.

Emanuel, K. A. (1991), A scheme for representing cumulus convection in large-scale models, *J. Atmos. Sci.*, **48**, 2312–2335.

Emanuel, K., and R. T. Pierrehumbert (1996), Microphysical and dynamical control of tropospheric water vapour, in *Clouds, Chemistry and Climate, NATO ASI Ser. I, Global Environ. Change*, vol. 35, edited by P. J. Crutzen and V. Ramanathan, pp. 17–28, Springer, New York.

Emanuel, K. A., and M. Živković-Rothman (1999), Development and evaluation of a convection scheme for use in climate models, *J. Atmos. Sci.*, **56**, 1766–1782.

Frierson, D. M. W. (2007), The dynamics of idealized convection schemes and their effect on the zonally averaged tropical circulation, *J. Atmos. Sci.*, **64**, 1959–1976.

Gettelman, A., W. Collins, E. Fetzer, A. Eldering, F. Irion, P. Duffy, and G. Bala (2006), Climatology of upper-tropospheric humidity from the Atmospheric Infrared Sounder and implications for climate, *J. Clim.*, **19**, 6104–6121.

Greenwald, T. J., and S. A. Christopher (2002), Effect of cold clouds on satellite measurements near 183 GHz, *J. Geophys. Res.*, **107**(D13), 4170, doi:10.1029/2000JD000258.

Held, I., and B. Soden (2000), Water vapour feedback and global warming, *Annu. Rev. Energy Environ.*, **25**, 441–475.

Hong, G., G. Heygster, J. Miao, and K. Kunzi (2005), Detection of tropical deep convective clouds from AMSU-B water vapor channels measurements, *J. Geophys. Res.*, **110**, D05205, doi:10.1029/2004JD004949.

Ingram, W. J. (2002), On the robustness of the water vapor feedback: GCM vertical resolution and formulation, *J. Clim.*, **15**, 917–921.

Kanamitsu, M., W. Ebisuzaki, J. Woollen, S.-K. Yang, J. J. Hnilo, M. Fiorino, and G. L. Potter (2002), NCEP-DEO AMIP-II reanalysis (R2), *Bull. Am. Meteorol. Soc.*, **83**, 1631–1643.

Larson, K., and D. Hartmann (2003), Interactions among cloud, water vapor, radiation, and large-scale circulation in the tropical climate. Part I: Sensitivity to uniform sea surface temperature changes, *J. Clim.*, **16**, 1425–1440.

Matricardi, M., F. Chevallier, G. Kelly, and J.-N. Thépaut (2004), An improved general fast radiative transfer model for the assimilation of radiance observations, *Q. J. R. Meteorol. Soc.*, **130**, 153–173.

Minschwaner, K., and A. Dessler (2004), Water vapor feedback in the tropical upper troposphere: Model results and observations, *J. Clim.*, **17**, 1272–1282.

Pierrehumbert, R. T. (1998), Lateral mixing as a source of subtropical water vapor, *Geophys. Res. Lett.*, **25**, 151–154.

Pierrehumbert, R. T., H. Brogniez, and R. Roca (2007), On the relative humidity of the Earth's atmosphere, in *The Global Circulation of the Atmosphere*, edited by T. Schneider and A. H. Sobel, pp. 143–185, Princeton Univ. Press, Princeton, N. J.

Sherwood, S. (1996), Maintenance of the free tropospheric tropical water vapor distribution. Part II: Simulation by large-scale advection, *J. Clim.*, **9**, 2919–2934.

Sherwood, S., and C. Meyer (2006), The general circulation and robust relative humidity, *J. Clim.*, **19**, 6278–6290.

Soden, B., and F. Bretherton (1993), Upper tropospheric relative humidity field from the GOES 6.7 μm channel: Method and climatology for July 1987, *J. Geophys. Res.*, **98**, 16,669–16,688.

Soden, B., and I. Held (2006), An assessment of climate feedbacks in coupled ocean-atmosphere models, *J. Clim.*, **19**, 3354–3360.

Soden, B., D. Jackson, V. Ramaswamy, M. Schwarzkopf, and X. Huang (2005), The radiative signature of Upper Tropospheric Moistening, *Science*, **310**, 841–844.

Spencer, R., and W. Braswell (1997), How dry is the tropical free troposphere?: Implications for a global warming theory, *Bull. Am. Meteorol. Soc.*, **78**, 1097–1106.

Tiedtke, M. (1989), A comprehensive mass flux scheme for cumulus parameterization in large-scale models, *Mon. Weather Rev.*, **117**, 1779–1800.

Uppala, S., et al. (2005), The ERA-40 re-analysis, *Q. J. R. Meteorol. Soc.*, **31**, 2961–3012.

Wyant, M., C. Bretherton, J. Bacmeister, J. Kiehl, I. Held, M. Zhao, S. Klein, and B. Soden (2006), A comparison of tropical cloud properties and responses in GCMs using mid-tropospheric vertical velocity, *Clim. Dyn.*, **27**, 261–279.

Zhang, G. J., and N. A. McFarlane (1995), Sensitivity of climate simulations to the parametrization of cumulus convection in the Canadian Climate Center general circulation model, *Atmos. Ocean*, **33**, 407–446.

H. Brogniez, Centre d'Etude des Environnements Terrestres et Planétaires, CNRS, IPSL, 10-12 avenue de l'Europe, F-78140 Velizy, France. (helene.brogniez@cetp.ipsl.fr)

R. T. Pierrehumbert, Department of Geophysical Sciences, University of Chicago, 5734 S. Ellis Avenue, Chicago, IL 60637, USA.